Journal of Molecular Science

Journal of Molecular Science
Volume 36 Issue 2, Year of Publication 2026, Page 540-548
DoI-10.004687/1000-9035.2026.064

Journal of Molecular Science
www.jmolecularsci.com ISSN:1000-9035

Formulation and Evaluation of Surface-Modified Nanostructured Lipid Carriers for Intranasal Brain Delivery of Cariprazine Hydrochloride

Shweta R. Jaiswal*, Veena S. Belgamwar
Department of Pharmaceutical Sciences, Rashtrasant Tukadoji Maharaj Nagpur University, Nagpur, Maharashtra, India

Article Information
Received: 07-04-2026
Revised: 21-06-2026
Accepted: 24-07-2026
Published: 28-07-2026

Keywords
Nanostructured lipid carriers, surface modification, coating, mucoadhesion, Cariprazine Hydrochloride

ABSTRACT

Background: Cariprazine hydrochloride (CRP), a third-generation atypical antipsychotic, exhibits limited oral bioavailability due to extensive first-pass metabolism, making intranasal delivery a promising alternative for enhancing drug delivery to the central nervous system. The present study aimed to design, develop, and evaluate chitosan-coated nanostructured lipid carriers (CRP-CS-NLCs) as a potential intranasal nanocarrier system for enhanced brain delivery of CRP. **Methods:** CRP-CS-NLCs were prepared by hot high-shear homogenization using Compritol® E ATO and oleic acid as the lipid matrix, Pluronic® F68 as the stabilizer, sodium deoxycholate as the co-surfactant, and low molecular weight chitosan as the mucoadhesive coating polymer. The formulations were characterized for particle size, zeta potential, entrapment efficiency, surface morphology, in vitro drug release, release kinetics, ex vivo permeation, mucoadhesion, and hemocompatibility. **Results:** The optimized formulation (F4) exhibited a particle size of 178.2 ± 1.2 nm, a PDI of 0.357, a positive zeta potential of +30.2 ± 1.2 mV, and an entrapment efficiency of 70.6 ± 1.4%. FE-SEM analysis revealed predominantly spherical nanoparticles with smooth surfaces. The formulation demonstrated sustained drug release over 48 h, with the Korsmeyer–Peppas model providing the best fit (R^2 = 0.9781). Ex vivo permeation studies demonstrated sustained transmucosal drug transport across the nasal mucosa. Mucoadhesion studies showed increased turbidity and particle size, together with a reduction in zeta potential following interaction with mucin, confirming effective mucoadhesive behavior. Hemolysis of <2% indicated excellent hemocompatibility of the optimized formulation. **Conclusion:** The developed CRP-CS-NLCs exhibited desirable physicochemical characteristics, sustained drug release, favorable ex vivo permeation, good mucoadhesive properties and hemocompatibility, indicating their potential as a promising intranasal drug delivery system for CRP. Further in vivo pharmacokinetic studies are warranted to establish their efficacy for nose-to-brain drug delivery.

©2026 The authors
This is an Open Access article distributed under the terms of the Creative Commons Attribution (CC BY NC), which permits unrestricted use, distribution, and reproduction in any medium, as long as the original authors and source are cited. No permission is required from the authors or the publishers.(https://creativecommons.org/licenses/by-nc/4.0/)

1. INTRODUCTION:

Schizophrenia is a severe and chronic neuropsychiatric disorder with a worldwide prevalence of millions of individuals, and is defined by positive symptoms, negative symptoms and cognitive impairment [1],[2]. Despite the advances in pharmacotherapy, long-term management is still difficult due to the need to administer the drugs for an extended period, and the lack of drug exposure at the site of action can play a role in the variability of therapeutic results [3]. In addition, effective treatment of central nervous system (CNS) disorders is intrinsically limited by the blood-brain barrier (BBB) which controls the delivery of therapeutic agents into the brain [4]. Thus, the design of novel

Journal of Molecular Science
Volume 36 Issue 2, Year of Publication 2026, Page 540-548
DoI-10.004687/1000-9035.2026.064

drug delivery systems that can facilitate the delivery of drugs to the CNS with reduced exposure in the systemic circulation has emerged as an important research area in the pharmaceutical industry [5].

Cariprazine hydrochloride (CRP) is an atypical antipsychotic drug of the third generation approved for the treatment of schizophrenia and other psychiatric disorders [6], [7]. It is a partial agonist of dopamine receptors (D_3/D_2) with a higher affinity for D_3 receptors, which leads to therapeutic effects on both the positive and negative symptoms of schizophrenia [8]. CRP, however, belongs to the Biopharmaceutics Classification System class II, which is defined to have low aqueous solubility and high membrane permeability [9], with formulation challenges that may impact its dissolution and drug availability after conventional oral administration. Furthermore, oral administration results in extensive hepatic metabolism, which results in systemic drug exposure prior to reaching the CNS [10]. These restrictions serve as a justification to investigate other formulations delivery methods that can enhance the formulation performance and can enable more efficient drug transport to the brain.

Intranasal delivery is one of the alternative routes being explored for CNS drug delivery that offers the potential of delivering therapeutic agents to the brain via the olfactory and trigeminal pathways, as well as by bypassing the BBB and avoiding hepatic first-pass metabolism [11], [12]. In addition to its potential to decrease systemic drug exposure, intranasal delivery provides for rapid drug absorption and patient acceptance. However, this route is often inefficient due to the rapid mucociliary clearance, degradation by the enzymes present in the nasal cavity and the short residence time of the conventional formulation, which requires that the formulation be designed to improve nasal retention and to work for a longer periods of time to achieve drug permeation [13].

Nanostructured lipid carriers (NLCs) have been the subject of significant research as an ideal nanocarrier for intranasal drug delivery due to their highly efficient drug loading capacity, ability to increase apparent drug solubility, controlled drug release and physicochemical stability. The imperfect lipid matrix of NLCs offers higher drug-loading capacity than conventional solid lipid nanoparticles while minimizing drug expulsion during storage. The small size and the lipid based composition allow them to come into close contact with the nasal mucous membrane and thus make them promising vectors for intranasal delivery of poorly water-soluble drugs for CNS action, like CRP [14]–[16].

Mucoadhesive polymers can be further used to modify the surface of nanocarriers, which would further increase their suitability for intranasal delivery. Chitosan is one of these polymers that has been extensively studied due to its intrinsic mucoadhesive properties, biodegradability, cationic nature and excellent biocompatibility [17], [18]. The electrostatic attraction between the positively charged amino groups of chitosan and the negatively charged mucin glycoproteins leads to a long residence time on the nasal mucosal surface [19]. Moreover, chitosan was reported to transiently regulate epithelial tight junctions, thus enhancing the paracellular transport of drugs through the nasal epithelium [20]. Therefore, the chitosan coated lipid nanocarriers are attractive candidates for intranasal delivery because of their ability to sustain the release of the drug, extend the residence time in nasal cavity and enhance interaction with the nasal mucosa.

Considering these factors, the present study aimed to design and characterize CRP -loaded chitosan-coated nanostructured lipid carriers (CRP-CS-NLCs) as a mucoadhesive intranasal drug delivery system. The developed formulation was tested for its physicochemical properties, drug entrapment efficiency, in vitro drug release pattern, ex vivo nasal permeation and mucoadhesive properties to explore its potential as an intranasal delivery platform. It was hypothesized that the integration of NLCs with a mucoadhesive chitosan coating would enhance formulation retention at the nasal mucosa, support sustained drug release and permeation, and thereby provide a promising platform for intranasal delivery of CRP with potential applicability for nose-to-brain drug delivery.

2. MATERIALS AND METHODS:

2.1 Chemicals and solvents:

Cariprazine hydrochloride was received as a gratis sample from MSN Laboratories pvt. ltd., Telangana, India. Compritol® E ATO was kindly provided as a gift sample by Gattefosse, India. Oleic acid, Chitosan, Pluronic® F68 and sodium deoxycholate were procured from Sigma-Aldrich. All other chemicals and solvents used in the study were of analytical grade.

2.2 Preparation of CRP-CS-NLCs:

CRP -loaded nanostructured lipid carriers (CRP-NLCs) were prepared using the hot high-shear homogenization technique [21]. The lipid phase consisted of Compritol® E ATO and oleic acid (80:20, w/w), which were melted at approximately 80 ± 2°C. CRP was incorporated into the molten lipid phase according to the specified drug-to-lipid ratio under continuous magnetic stirring until a homogeneous mixture was obtained. The aqueous phase, containing Pluronic® F68 (0.4–0.8%, w/v)

Journal of Molecular Science
Volume 36 Issue 2, Year of Publication 2026, Page 540-548
DoI-10.004687/1000-9035.2026.064

and sodium deoxycholate (0.15%, w/v), was heated to the same temperature as the lipid phase. The hot aqueous phase was gradually added to the molten lipid phase under high-shear homogenization using an Ultra-Turrax® T18 homogenizer (IKA, Germany) operated at 12,000 rpm for 20 min to produce nanoemulsion. The resulting dispersion was cooled to room temperature under continuous magnetic stirring, leading to recrystallization of the lipid matrix and formation of CRP-NLCs.

For surface modification, an aqueous chitosan solution (0.1%, w/v) was prepared by dissolving chitosan in 1% (v/v) acetic acid with continuous stirring overnight. Equal volumes of the optimized NLC dispersion and chitosan solution were mixed by adding the NLC dispersion dropwise into the chitosan solution under gentle magnetic stirring for 30 min, allowing electrostatic adsorption of chitosan onto the negatively charged nanoparticle surface [22]. The resulting CRP-CS-NLCs were isolated by centrifugation at 15,000 rpm for 30 min, and the obtained pellet was washed and redispersed in distilled water and stored at 4°C until further characterization.

2.3 Particle Size and Zeta Potential:
The mean particle size, polydispersity index, and zeta potential of the CRP-CS-NLCs were determined by dynamic light scattering using a Nanopartica SZ-100 particle analyzer (Horiba Scientific, Kyoto, Japan). Before analysis, the nanoparticle dispersion was appropriately diluted with distilled water (approximately 1:10 dilution) to minimize multiple light scattering and ensure accurate measurements. All analyses were carried out at 25 ± 1 °C, and each sample was measured in triplicate. The results are presented as mean ± standard deviation.

2.4 Entrapment Efficiency:
The entrapment efficiency (EE) of the prepared CRP-CS-NLCs was determined by separating the unentrapped drug from the nanoparticle dispersion using refrigerated centrifugation. Briefly, the formulation was centrifuged at 18,000 rpm for 60 min at 4 °C. Following centrifugation, the supernatant containing the free (unentrapped) drug was carefully collected and determined using UV–visible spectrophotometric method at 244.5 nm. The EE was calculated using the following equation:

$$EE\ (\%) = \frac{\text{Total drug} - \text{Free drug}}{\text{Total drug}}\ x\ 100$$

where Total drug represents the amount of CRP initially incorporated into the formulation, and Free drug corresponds to the amount of unentrapped drug present in the supernatant. All measurements were performed in triplicate, and the results are expressed as mean ± standard deviation.

2.5 Surface Morphology by Field Emission Scanning Electron Microscopy (FE-SEM):
The surface morphology of the optimized CRP-CS-NLCs was examined using FE-SEM. A small volume (10 µL) of the optimized formulation was placed onto an aluminum stub using double-sided conductive carbon tape and allowed to dry under vacuum. The dried sample was sputter-coated with a thin layer of gold to improve electrical conductivity prior to imaging. FE-SEM analysis was performed at an accelerating voltage of 5 kV using appropriate magnifications to evaluate the particle morphology and surface characteristics.

2.6 In Vitro Drug Release Study:
The in vitro release behavior of CRP-CS-NLCs was evaluated using a Franz diffusion cell equipped with a dialysis membrane of molecular weight cut-off 12–14 kDa [23]. The donor compartment was loaded with the optimized CRP-CS-NLC formulation containing an amount equivalent to 1 mg of CRP, while the receptor compartment was filled with simulated nasal fluid (SNF) maintained at 37 ± 0.5°C under continuous magnetic stirring at 50 rpm. At predetermined intervals (0, 0.5, 1, 2, 4, 6, 8, 10, 12, 18, 24, 36, and 48 h), 1 mL of the receptor medium was withdrawn and immediately replenished with an equal volume of fresh SNF to maintain sink conditions throughout the study. The collected samples were analyzed using a UV–Visible spectrophotometer (Shimadzu UV-1800, Japan) at 244.5 nm, and the cumulative percentage drug release was calculated. All experiments were performed in triplicate, and the results are expressed as mean ± standard deviation.

2.7 Drug Release Kinetics:
The in vitro drug release data of the optimized CRP-CS-NLC formulation were fitted to different kinetic models, including zero-order, first-order, Higuchi, and Korsmeyer–Peppas models, to elucidate the drug release mechanism. The model showing the highest correlation coefficient (R^2) was considered to best describe the release behavior. Furthermore, the release exponent (n) obtained from the Korsmeyer–Peppas model was used to determine the mechanism of drug release from the NLC system.

2.8 Ex Vivo Permeation Study:
The ex vivo permeation study of the optimized CRP-CS-NLCs was carried out using freshly excised goat nasal mucosa procured from a local slaughterhouse. The excised mucosal tissue was carefully cleaned with normal saline to remove adhering mucus and other extraneous materials before being mounted between the donor and receptor compartments of a Franz diffusion cell, with the mucosal surface facing the donor compartment. The receptor compartment was filled with SNF (pH 6.4) and maintained at 37 ±

Journal of Molecular Science
Journal of Molecular Science
Volume 36 Issue 2, Year of Publication 2026, Page 540-548
DoI-10.004687/1000-9035.2026.064

0.5°C under continuous magnetic stirring. An accurately measured amount of the optimized CRP-CS-NLC formulation equivalent was placed in the donor compartment. At predetermined time intervals, 1 mL aliquots were withdrawn from the receptor compartment and immediately replaced with an equal volume of fresh preheated SNF to maintain sink conditions throughout the study [24]. The collected samples were suitably analyzed using a UV–Visible spectrophotometer (UV-1900, Shimadzu, Japan) at 244.5 nm in triplicates, and the data is displayed as mean ± standard deviation

2.9 In vitro mucoadhesion study:

The mucoadhesive properties of the optimized CRP-CS-NLCs were evaluated using a turbidimetric method in combination with mucin–nanoparticle interaction studies. A 0.08% (w/v) mucin dispersion was prepared in ultrapure water by continuous stirring overnight at room temperature and subsequently equilibrated at 37 ± 0.5 °C. Prior to use, the mucin dispersion was centrifuged at 6000 rpm for 10 min to remove any undissolved particles. The optimized CS-NLC formulation was mixed with the mucin dispersion in a 2:1 (v/v) ratio using a vortex mixer for 1 min and incubated at 37 ± 0.5 °C. The interaction between the nanoparticles and mucin was evaluated at 0, 30, and 60 min. The turbidity of the mixtures was determined by measuring the absorbance at 650 nm using a UV–Visible spectrophotometer, with mucin dispersion serving as the reference. To further investigate the interaction between the nanoparticles and mucin, the mean particle size and zeta potential of the CRP-CS-NLCs were measured before and after incubation with mucin at the predetermined time intervals using a dynamic light scattering analyzer (Nanopartica SZ-100, Horiba Scientific, Kyoto, Japan). Changes in turbidity, particle size, and zeta potential were used as indicators of mucoadhesive interaction between the chitosan-coated nanoparticles and mucin[25].

2.10 Hemolytic Toxicity Study:

The hemocompatibility of the optimized CRP-CS-NLCs was evaluated using freshly collected blood from healthy Wistar rats. Red blood cells (RBCs) were isolated and washed with normal saline (0.9% w/v), followed by preparation of a 2% (v/v) RBC suspension in saline. An aliquot of 100 µL of the formulation was mixed with 900 µL of the RBC suspension and incubated at 37 ± 2 °C for 1 h. Normal saline (0.9% w/v) and 1% (v/v) Triton X-100 were used as the negative (0% hemolysis) and positive (100% hemolysis) controls, respectively. Following incubation, the samples were centrifuged at 4477 × g for 10 min, and the absorbance of the supernatant was measured at 545 nm using a UV–Visible spectrophotometer. The percentage hemolysis was calculated using the following equation [26]:

$$\%Hemolysis = \frac{Absorbance\ of\ Sample - Absorbance\ of\ Negative\ Control}{Absorbance\ of\ Positive\ Control - Absorbance\ of\ Negative\ Control} x\ 100$$

RESULTS AND DISCUSSION:

3.1 Formulation Development of CRP-CS-NLCs:

Various formulations of CRP-NLCs were prepared by varying the total lipid concentration, surfactant concentration (Pluronic® F68), and drug-to-lipid ratio while maintaining a constant Compritol® E ATO to oleic acid ratio (80:20, w/w). Sodium deoxycholate (0.15%, w/v) was incorporated into all formulations to provide a negative surface charge and improve nanoparticle stability. The uncoated NLCs were subsequently coated with low molecular weight chitosan to obtain CRP-CS-NLCs. Compritol® E ATO was chosen as the solid lipid owing to the stability of the lipid matrix and sustained drug release ability, while oleic acid was used as the liquid lipid in order to improve drug incorporation into the imperfect lipid matrix [27]. Pluronic® F68 was employed as a stabilizer to reduce interfacial tension during homogenization and to prevent aggregation of nanoparticles. Sodium deoxycholate was incorporated as a co-surfactant to impart a negative surface charge, thereby improving the physical stability of the nanoparticles and facilitating subsequent electrostatic coating with chitosan. The coating with chitosan was carried out to provide mucoadhesive property to the formulation, which may prolong nasal residence time and improve nose-to-brain delivery of CRP [28]. The composition of all formulations is shown in Table 1. The developed formulations were evaluated for particle size, zeta potential, and entrapment efficiency. Based on these physicochemical parameters, the optimized formulation was chosen.

Table 1. Formulation composition and physicochemical properties of CRP-CS-NLCs

Batch	Drug:Lipid Ratio	Total Lipid (% w/v)	Pluronic F68 (% w/v)	Particle Size (nm)	Zeta Potential (mV)	Entrapment Efficiency (%)
F1	1:10	1.5	0.4	188.4 ± 2.1	+25.4 ± 1.2	55.8 ± 1.6
F2	1:10	2.0	0.4	206.7 ± 1.8	+26.6 ± 1.1	66.4 ± 1.5
F3	1:10	2.0	0.6	176.3 ± 1.5	+28.7 ± 1.0	61.9 ± 1.8
F4	**1:15**	**2.0**	**0.6**	**178.2 ± 1.2**	**+30.2 ± 1.2**	**70.6 ± 1.4**
F5	1:15	2.5	0.6	198.6 ± 1.7	+30.5 ± 1.1	72.4 ± 1.3
F6	1:15	2.0	0.8	170.8 ± 1.4	+28.9 ± 1.2	62.2 ± 1.5

3.2 Particle Size and Zeta Potential:

Particle size and zeta potential of CRP-CS-NLC

Journal of Molecular Science
Volume 36 Issue 2, Year of Publication 2026, Page 540-548
DoI-10.004687/1000-9035.2026.064

formulations are shown in Table 1. The average particle size of chitosan-coated formulations was found between 170.8 ± 1.4 nm and 206.7 ± 1.8 nm, indicating the successful production of nanoparticles with desirable size suitable for intranasal administration. Nanoparticles less than 200 nm in diameter are regarded as preferable for their nasal absorption and transport via olfactory and trigeminal routes[29]. Increasing the total concentration of lipid from 1.5 to 2.0% w/v (F1 to F2), with constant concentration of surfactant, led to increase in particle size from 188.4 ± 2.1 nm to 206.7 ± 1.8 nm. This increment in particle size could be due to the increased viscosity of the lipid phase that lowers the homogenization efficiency, thus leading to the formation of larger emulsion droplets. However, an increase in the concentration of Pluronic® F68 from 0.4 to 0.6% w/v (F2 to F3) led to decrease in the particle size to 176.3 ± 1.5 nm because of better interfacial tension reduction and emulsion droplet stabilization during the homogenization process [30]. An increase in the drug: lipid ratio from 1:10 to 1:15 (from F3 to F4) showed a slight increase in the nanoparticle size of 178.2 ± 1.2 nm, which could be because of the availability of more amount of lipids for drug entrapment. A further increase in the total lipid concentration to 2.5% w/v (F5) resulted in an increase in the particle size to 198.6 ± 1.7 nm, while increasing the surfactant concentration to 0.8% w/v (F6) resulted in the smallest nanoparticles of 170.8 ± 1.4 nm due to improved emulsification and stabilization.

All formulations showed positive zeta potential values between +25.4 ± 1.2 mV and +30.5 ± 1.1 mV, indicating successful coating of nanoparticles with chitosan. The presence of positive surface charge is explained by the protonation of amino groups of chitosan that adsorbed on the surface of negatively charged nanoparticles. Since the concentration of chitosan and conditions of coating were kept constant throughout the experiment, the variations in zeta potential were insignificant. These small changes may be explained by variations in composition of lipids and surfactants, which might affect the amount of adsorption of chitosan on the surface of nanoparticles. Positive zeta potential is expected to enhance electrostatic interaction with negatively charged surface of nasal mucosa, thus enhancing mucoadhesion of the formulation and prolonging its retention in the nasal cavity. [31]. Out of all formulations, F4 demonstrated a particle size of 178.2 ± 1.2 nm, polydispersity index of 0.357, showing relatively homogeneous distribution of particles, as well as a positive zeta potential of +30.2 ± 1.2 mV. The particle size distribution and zeta potential profile of F4 are shown in Figure 1(A) and (B), respectively. Based on its balanced physicochemical characteristics, F4 was selected for subsequent characterization and further in vitro studies.

3.3 Entrapment Efficiency:

The EE of the developed CRP-CS-NLC formulations is presented in Table 1 and ranged from 55.8 ± 1.6% to 72.4 ± 1.3%. The obtained entrapment efficiencies demonstrate the ability of the NLCs to incorporate CRP within the lipid matrix. An increase in the total lipid concentration from 1.5 to 2.0% w/v (F1 to F2) improved the EE from 55.8 ± 1.6% to 66.4 ± 1.5%, which may be attributed to the greater lipid matrix available for accommodating the drug. However, increasing the concentration of Pluronic® F68 from 0.4 to 0.6% w/v (F2 to F3) resulted in a reduction in EE to 61.9 ± 1.8%. This decrease may be explained by the increased solubilization of CRP in the aqueous phase at higher surfactant concentrations, leading to greater partitioning of the drug outside the lipid matrix during nanoparticle formation. Increasing the drug-to-lipid ratio from 1:10 to 1:15 (F3 to F4) markedly improved the EE to 70.6 ± 1.4%, indicating that a greater proportion of lipid relative to drug provides additional space within the imperfect lipid matrix for efficient drug incorporation [32]. A further increase in the total lipid concentration (F5) produced the highest EE (72.4 ± 1.3%), although this was accompanied by an increase in particle size. Increasing the surfactant concentration to 0.8% w/v (F6) again reduced the EE to 62.2 ± 1.5%, which may be attributed to enhanced drug partitioning into the aqueous phase.

Although formulation F5 exhibited the highest entrapment efficiency, formulation F4 was selected as the optimized formulation because it provided the best balance between particle size, surface charge, and drug entrapment, making it more suitable for intranasal nose-to-brain delivery.

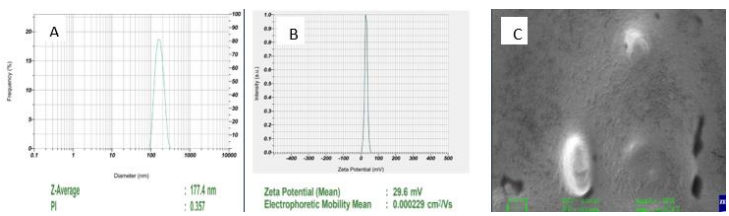

Figure 1. (A) Particle size of F4, (B) Zeta potential of F4 and (C) FE-SEM micrograph of F4

3.4 Surface Morphology by FE-SEMS:

The surface morphology of the optimized CRP-CS-

Journal of Molecular Science
Volume 36 Issue 2, Year of Publication 2026, Page 540-548
DoI-10.004687/1000-9035.2026.064

NLCs was examined by FE-SEM, and the representative micrograph is presented in Figure 1(C). The nanoparticles exhibited predominantly spherical to near-spherical morphology with well-defined particle boundaries, indicating the successful formation of NLCs. The particles appeared discrete and well dispersed in the observed field without any evident aggregation. The surface of the nanoparticles appeared smooth, and the nanoscale morphology was consistent with the particle size obtained from dynamic light scattering, further confirming the successful preparation of the CRP-CS-NLC formulation suitable for intranasal drug delivery.

3.5 In Vitro Drug Release Study:

The in vitro release profile of the optimized CRP-CS-NLCs is presented in Figure 2(A). The formulation exhibited a biphasic release pattern characterized by an initial burst release followed by a sustained release phase. Approximately 9.92% of the drug was released within the first 30 min, which increased to 22.74% after 2 h. It is believed that the initial burst is caused by the release of drug molecules either adsorbed or attached to the surface of the nanoparticle. Afterward, there was controlled drug release, reaching 37.12%, 51.99%, and 65.54% at 6, 10, and 24 hours, respectively. In terms of the optimized formulation, the cumulative percentage drug release after 48 hours was found to be 84.22%, implying that there was prolonged CRP release from the lipid matrix. This sustained release behavior can be attributed to the gradual diffusion of the drug through the solid–liquid lipid matrix, along with the presence of the chitosan coating barrier, which reduces the rate of drug diffusion into the release medium [33], [34]. The sustained release profile observed for the optimized CRP-CS-NLC formulation is considered advantageous for intranasal application, as prolonged drug release may enhance nasal residence time and maintain therapeutic drug concentrations over an extended period [35], thereby potentially improving nose-to-brain delivery of CRP.

3.6 Drug Release Kinetics:

The in vitro release data of the optimized CRP-CS-NLC formulation were fitted to various mathematical models to elucidate the mechanism of drug release, and the obtained kinetic parameters are presented in Table 2. Among the models evaluated, the Korsmeyer–Peppas model exhibited the highest correlation coefficient (R^2 = 0.9781), followed by the Higuchi model (R^2 = 0.9624), indicating that the release of CRP from the CRP-CS-NLC was predominantly governed by diffusion through the lipid matrix. In comparison, the first-order (R^2 = 0.9475) and zero-order (R^2 = 0.8309) models showed relatively lower correlation coefficients. The release exponent (n = 0.4591) obtained from the Korsmeyer–Peppas model indicated an anomalous release mechanism, suggesting that drug release was governed by a combination of diffusion through the lipid matrix and relaxation of the hydrated chitosan coating [36]. The sustained release profile is therefore attributed to the combined influence of the lipid matrix and the chitosan coating, which together regulate drug diffusion into the release medium [37]. These findings are in agreement with the sustained release profile obtained for the optimized CRP-CS-NLC formulation and support its potential application for prolonged intranasal drug delivery.

Table 2. Kinetic modelling parameters for the in vitro release of CRP-CS-NLC formulation.

Model	R^2
Zero-order	0.8309
First-order	0.9475
Higuchi	0.9624
Korsmeyer–Peppas	**0.9781**
Release exponent (n)	**0.4591**

3.7 Ex Vivo Permeation Study:

The ex vivo permeation behavior of the optimized CRP-CS-NLCs was evaluated across excised sheep nasal mucosa using a Franz diffusion cell over 48 h. The formulation exhibited a sustained and progressive permeation profile without an excessive initial burst. The cumulative drug permeation increased from 3.95% at 0.5 h to 19.8% at 4 h, followed by a gradual increase to 40.2% at 12 h, ultimately reaching 63.2% after 48 h as shown in Figure 2(B). The almost linear permeation profile obtained during the steady-state phase is an indication that the drug was continuously diffusing through the nasal membrane. Analysis of the steady-state permeation phase using linear regression gave the steady-state flux (Jss) value as 6.52 μg/cm^2/h. From the donor concentration at the beginning (200 μg/mL), the permeability coefficient (Kp) value of 0.0326 cm/h was obtained, showing that CRP was efficiently diffused through the nasal membrane. The sustained permeation profile can be attributed to the NLC matrix, which provided controlled drug release while maintaining a favorable concentration gradient across the membrane. Furthermore, the chitosan coating likely enhanced the interaction of the nanoparticles with the nasal mucosa through its mucoadhesive properties and transient modulation of tight junctions, thereby facilitating prolonged drug permeation [38], [39]. Collectively, these findings indicate that the optimized CRP-CS-NLC formulation provides sustained transmucosal drug transport and support their suitability as a promising intranasal nose-to-brain drug delivery system.

Journal of Molecular Science
Journal of Molecular Science
Volume 36 Issue 2, Year of Publication 2026, Page 540-548
DoI-10.004687/1000-9035.2026.064

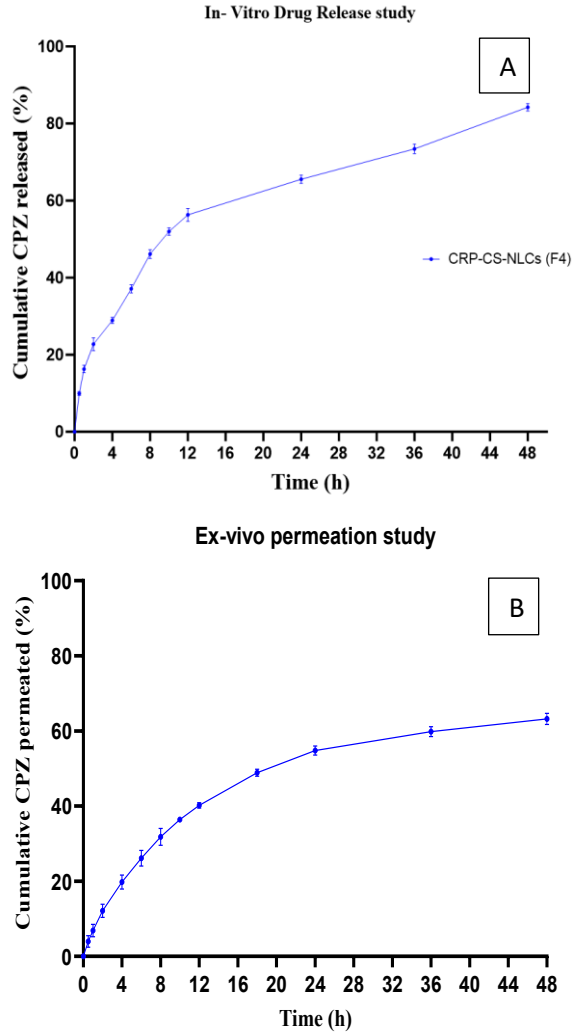

Figure 2. (A) In vitro release profile of F4 and (B) Ex vivo nasal permeation profile of F4

3.8 Mucoadhesion Study:

The mucoadhesive behavior of the optimized CRP-CS-NLCs was evaluated by monitoring changes in turbidity, particle size, and zeta potential following incubation with mucin. As shown in Figure 3, the absorbance of the CRP-CS-NLCs –mucin dispersion exhibited a gradual increase with incubation time and remained consistently higher than that of the CRP-CS-NLCs dispersion in water. The mucin dispersion alone showed the lowest absorbance throughout the study. These findings indicate enhanced interaction between the chitosan-coated nanoparticles and mucin, confirming the mucoadhesive nature of the formulation [40]. The mean particle size of the CRP-CS-NLCs increased from 176.2 ± 1.2 nm before incubation to 189.2 ± 2.1 nm and 212.5 ± 2.3 nm after 30 and 60 min of incubation with mucin, respectively. The increase in particle size suggested the adsorption of mucin onto the nanoparticle surface, resulting in the formation of a mucoadhesive layer. Similarly, the zeta potential of the optimized CRP-CS-NLCs decreased from +30.2 ± 0.7 mV to +20.7 ± 1.1 mV after interaction with mucin. This reduction in surface charge is attributed to electrostatic interactions between the positively charged amino groups of chitosan and the negatively charged sialic acid and sulfate residues present in mucin glycoproteins [41]. The particles, however, retained a positive surface charge after incubation, indicating that the interaction with mucin did not compromise the colloidal stability of the formulation. Overall, the observed increase in turbidity and particle size, together with the reduction in zeta potential, confirmed successful interaction between the chitosan-coated nanostructured lipid carriers and mucin, demonstrating the mucoadhesive characteristics of the optimized formulation. Such mucoadhesive behavior is expected to prolong the residence time of the formulation within the nasal cavity, thereby supporting improved intranasal drug delivery.

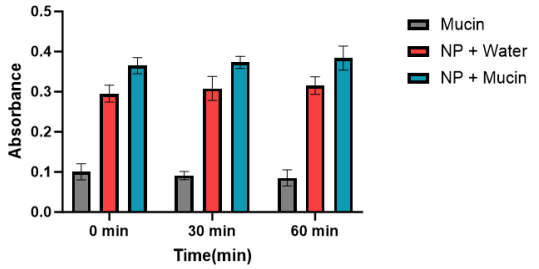

Figure 3. Absorbance values of CRP-CS-NLCs after interaction with water and mucin at 650 nm as a function of time

3.9 Hemolytic Toxicity Study:

Hemocompatibility was determined on the basis of the percentage of RBCs hemolysis in the presence of the optimized CRP-CS-NLC formulation. The optimized CS-NLCs showed a percentage hemolysis of < 2%, signifying very little damage to erythrocytes. Materials that induce less than 5% hemolysis are classified as non-hemolytic and are deemed suitable for biomedical applications [42]. The obtained hemolysis level was far below this value, hence supporting the high hemocompatibility of the developed formulation. The low level of hemolysis can be associated with the biocompatibility of the lipid constituents of the NLCs and the chitosan coating, which reduce membrane disruption upon contact with erythrocytes [43]. These results indicate that the developed CRP-CS-NLC formulation is blood compatible, supporting its potential use as a safe intranasal drug delivery system.

4. CONCLUSION:

In the current study, chitosan-coated nanostructured lipid carriers loaded with CRP were successfully designed and investigated as a promising delivery

Journal of Molecular Science
Volume 36 Issue 2, Year of Publication 2026, Page 540-548
DoI-10.004687/1000-9035.2026.064

system for intranasal drug delivery. The optimized system exhibited favorable physicochemical properties including small particles' size, narrow size distribution, adequate surface charge, and high drug loading efficiency. Sustained drug release was observed in vitro while higher drug permeability across nasal mucosa was noted during ex vivo studies. Moreover, the prepared formulation also exhibited good mucoadhesive ability as seen by its enhanced interaction with mucin. The current formulation also exhibited excellent biocompatibility and proper surface morphology, confirming its safety and compatibility for intranasal use. Overall, the results indicate that chitosan-coated nanostructured lipid carriers offer a promising approach for the intranasal delivery of CRP by integrating sustained drug release, improved nasal permeation, and extended mucosal residence. However, further in vivo studies are necessary to confirm their potential for effective nose-to-brain drug delivery.

ACKNOWLEDGEMENT:
Authors would like to acknowledge the NFOBC Fellowship awarded to Shweta R. Jaiswal from Government of India, Ministry of Social Justice and Empowerment.

CONFLICTS OF INTERSEST:
The authors declare no conflict of interest.

REFERENCES:

1. S. J. Millard, C. E. Bearden, K. H. Karlsgodt, and M. J. Sharpe, "The prediction-error hypothesis of schizophrenia: new data point to circuit-specific changes in dopamine activity," *Neuropsychopharmacology*, vol. 47, no. 3, pp. 628–640, Feb. 2022.
2. C. U. Correll and N. R. Schooler, "Negative symptoms in schizophrenia: A review and clinical guide for recognition, assessment, and treatment," *Neuropsychiatr. Dis. Treat.*, vol. 16, pp. 519–534, Feb. 2020.
3. J. M. Kane and C. U. Correll, "Pharmacologic treatment of schizophrenia," *Dialogues Clin. Neurosci.*, vol. 12, no. 3, pp. 345–357, 2010.
4. D. Wu, Q. Chen, X. Chen, F. Han, Z. Chen, and Y. Wang, "The blood-brain barrier: structure, regulation, and drug delivery," *Signal Transduct. Target. Ther.*, vol. 8, no. 1, p. 217, May 2023.
5. S. V. Dhuria, L. R. Hanson, and W. H. Frey 2nd, "Intranasal delivery to the central nervous system: mechanisms and experimental considerations," *J. Pharm. Sci.*, vol. 99, no. 4, pp. 1654–1673, Apr. 2010.
6. L. Citrome, "Cariprazine: chemistry, pharmacodynamics, pharmacokinetics, and metabolism, clinical efficacy, safety, and tolerability," *Expert Opin. Drug Metab. Toxicol.*, vol. 9, no. 2, pp. 193–206, Feb. 2013.
7. I. Laszlovszky, Á. Barabássy, and G. Németh, "Cariprazine, A broad-spectrum antipsychotic for the treatment of schizophrenia: Pharmacology, efficacy, and safety," *Adv. Ther.*, vol. 38, no. 7, pp. 3652–3673, July 2021.
8. A. Wesołowska, A. Partyka, M. Jastrzębska-Więsek, and M. Kołaczkowski, "The preclinical discovery and development of cariprazine for the treatment of schizophrenia," *Expert Opin. Drug Discov.*, vol. 13, no. 8, pp. 779–790, Aug. 2018.
9. "Reagila (Cariprazine): European Public Assessment Report (EPAR). 2017. (Used for the BCS class II physicochemical information)," *European Medicines Agency*.
10. A. Periclou, L. Phillips, P. Ghahramani, M. Kapás, T. Carrothers, and T. Khariton, "Population Pharmacokinetics of Cariprazine and its Major Metabolites," *Eur. J. Drug Metab. Pharmacokinet.*, vol. 46, no. 1, pp. 53–69, Jan. 2021.
11. M. L. Formica, D. A. Real, M. L. Picchio, E. Catlin, R. F. Donnelly, and A. J. Paredes, "On a highway to the brain: A review on nose-to-brain drug delivery using nanoparticles," *Appl. Mater. Today*, vol. 29, no. 101631, p. 101631, Dec. 2022.
12. T. P. Crowe and W. H. Hsu, "Evaluation of recent intranasal drug delivery systems to the central nervous system," *Pharmaceutics*, vol. 14, no. 3, p. 629, Mar. 2022.
13. L. Illum, "Nasal drug delivery--possibilities, problems and solutions," *J. Control. Release*, vol. 87, no. 1–3, pp. 187–198, Feb. 2003.
14. R. H. Müller, M. Radtke, and S. A. Wissing, "Nanostructured lipid matrices for improved microencapsulation of drugs," *Int. J. Pharm.*, vol. 242, no. 1–2, pp. 121–128, Aug. 2002.
15. S. Khan, A. Sharma, and V. Jain, "An overview of nanostructured Lipid Carriers and its application in drug delivery through different routes," *Adv. Pharm. Bull.*, vol. 13, no. 3, pp. 446–460, July 2023.
16. R. H. Müller, R. Shegokar, and C. M. Keck, "20 years of lipid nanoparticles (SLN & NLC): present state of development and industrial applications," *Curr Drug Discov Technol*, vol. 8, no. 3, pp. 207–227, 2011.
17. L. Casettari and L. Illum, "Chitosan in nasal delivery systems for therapeutic drugs," *J. Control. Release*, vol. 190, pp. 189–200, Sept. 2014.
18. P. Mura, F. Maestrelli, M. Cirri, and N. Mennini, "Multiple roles of chitosan in mucosal drug delivery: An updated review," *Mar. Drugs*, vol. 20, no. 5, p. 335, May 2022.
19. L. Illum, "Chitosan and its use as a pharmaceutical excipient," *Pharm. Res.*, vol. 15, no. 9, pp. 1326–1331, Sept. 1998.
20. G. Kaur *et al.*, "Unraveling the role of chitosan for nasal drug delivery systems: A review," *Carbohydrate Polymer Technologies and Applications*, vol. 5, no. 100316, p. 100316, June 2023.
21. A. Patel and A. Dharamsi, "Voriconazole loaded lipidic nanoparticles for ophthalmic delivery: Development using QbD combined with risk-based approach," *Curr. Nanomed.*, vol. 13, no. 1, pp. 56–69, Mar. 2023.
22. A. Kapoor, A. Hafeez, P. Kushwaha, and N. Ara, "Chitosan-coated nanostructured lipid carriers of amantadine for nose-to-brain delivery: formulation optimization, in vitro-ex vivo characterization, and in vivo anti-parkinsonism assessment," *Int. J. Biol. Macromol.*, vol. 316, no. Pt 2, p. 144497, June 2025.
23. R. G. Madane and H. S. Mahajan, "Curcumin-loaded nanostructured lipid carriers (NLCs) for nasal administration: design, characterization, and in vivo study," *Drug Deliv.*, vol. 23, no. 4, pp. 1326–1334, May 2016.
24. M. Rahamathulla *et al.*, "Design and optimization of intranasal aripiprazole-loaded nanostructured lipid carriers for enhanced brain targeting in schizophrenia: in vitro and ex vivo evaluation," *Sci. Rep.*, vol. 15, no. 1, p. 45118, Dec. 2025.
25. A. Mehandole *et al.*, "Dasatinib loaded mucoadhesive lecithin-chitosan hybrid nanoparticles for its augmented oral delivery, in-vitro efficacy and safety," *Int. J. Pharm.*, vol. 651, no. 123784, p. 123784, Feb. 2024.
26. S. Sinha, P. R. Ravi, K. Prathmesh, and B. Ghosh, "Acalabrutinib loaded nanostructured lipid carriers to improve the oral delivery of the drug: Optimization, physicochemical characterization, in vivo pharmacokinetics and lymphatic uptake studies," *J. Drug Deliv. Sci. Technol.*, vol. 110, no. 107100, p. 107100, Aug. 2025.
27. S. Doktorovova, E. B. Souto, and A. M. Silva, "Nanotoxicology applied to solid lipid nanoparticles and nanostructured lipid carriers-A systematic review of in vitro

Journal of Molecular Science
Volume 36 Issue 2, Year of Publication 2026, Page 540-548
DoI-10.004687/1000-9035.2026.064

data," *European Journal of Pharmaceutics and Biopharmaceutics*, 2014.
28. D. Gadhave, "Chitosan-based mucoadhesive nanocarriers for intranasal drug delivery: Recent advances and future perspectives," *International Journal of Biological Macromolecules*, 2021.
29. P. G. Djupesland, "Nasal drug delivery devices: characteristics and performance in a clinical perspective-a review," *Drug Deliv. Transl. Res.*, vol. 3, no. 1, pp. 42–62, Feb. 2013.
30. N. Naseri, H. Valizadeh, and P. Zakeri-Milani, "Solid lipid nanoparticles and nanostructured lipid carriers: Structure, preparation and application," *Adv. Pharm. Bull.*, vol. 5, no. 3, pp. 305–313, Sept. 2015.
31. T. M. M Ways, W. M. Lau, and V. V. Khutoryanskiy, "Chitosan and its derivatives for application in mucoadhesive drug delivery systems," *Polymers (Basel)*, vol. 10, no. 3, p. E267, Mar. 2018.
32. J. Pardeike, A. Hommoss, and R. H. Müller, "Lipid nanoparticles (SLN, NLC) in cosmetic and pharmaceutical dermal products," *Int. J. Pharm.*, vol. 366, no. 1–2, pp. 170–184, Jan. 2009.
33. W. Mehnert and K. Mäder, "Solid lipid nanoparticles: production, characterization and applications," *Adv. Drug Deliv. Rev.*, vol. 47, no. 2–3, pp. 165–196, Apr. 2001.
34. U. Das, D. U. Kapoor, S. Singh, and B. G. Prajapati, "Unveiling the potential of chitosan-coated lipid nanoparticles in drug delivery for management of critical illness: a review," *Z. Naturforsch. C*, vol. 79, no. 5–6, pp. 107–124, May 2024.
35. W. Alwahsh, S. Sahudin, H. Alkhatib, M. F. Bostanudin, and M. Alwahsh, "Chitosan-based nanocarriers for pulmonary and intranasal drug delivery systems: A comprehensive overview of their applications," *Curr. Drug Targets*, vol. 25, no. 7, pp. 492–511, 2024.
36. J. Siepmann and F. Siepmann, "Mathematical modeling of drug dissolution," *Int. J. Pharm.*, vol. 453, no. 1, pp. 12–24, Aug. 2013.
37. A. C. Mendes, "Chitosan-coated lipid nanocarriers for controlled drug delivery: formulation strategies and release behavior," *International Journal of Biological Macromolecules*, 2023.
38. H. Omidian, E. J. Gill, and S. D. Chowdhury, "Recent advances in chitosan-based nanocarriers for intranasal drug delivery to the brain," *International Journal of Biological Macromolecules*, vol. 16, 2023.
39. S. Sharma, A. Verma, and S. K. Singh, "Recent advances in chitosan-based nanocarriers for intranasal drug delivery to the brain," *International Journal of Biological Macromolecules*, 2023.
40. A. Hakim, "Mucoadhesive chitosan-based nanosystems for intranasal drug delivery: Recent advances and characterization strategies," *International Journal of Biological Macromolecules*, 2023.
41. H. Omidian, E. J. Gill, S. Dey Chowdhury, and L. X. Cubeddu, "Chitosan nanoparticles for intranasal drug delivery," *Pharmaceutics*, vol. 16, no. 6, p. 746, May 2024.
42. "Standard recommended practice for the assessment of the hemolytic properties of materials," *Artif. Organs*, vol. 2, no. 3, pp. 318–320, Aug. 1978.
43. A. Tkachenko, "Hemocompatibility studies in nanotoxicology: Hemolysis or eryptosis? (A review)," *Toxicol. In Vitro*, vol. 98, no. 105814, p. 105814, June 2024.